Arctic moisture source for Eurasian snow cover variations in autumn

2015 Environ. Res. Lett. 10 054015

(http://iopscience.iop.org/1748-9326/10/5/054015)

Environmental Research Letters

LETTER

Arctic moisture source for Eurasian snow cover variations in autumn

Martin Wegmann[1], Yvan Orsolini[2], Marta Vázquez[3], Luis Gimeno[3], Raquel Nieto[3], Olga Bulygina[4], Ralf Jaiser[5], Dörthe Handorf[5], Annette Rinke[5], Klaus Dethloff[5], Alexander Sterin[4] and Stefan Brönnimann[1]

[1] Oeschger Centre for Climate Change Research and Institute of Geography, University of Bern, Switzerland
[2] NILU—Norwegian Institute for Air Research, Kjeller, Norway
[3] EPhysLab, Facultade de Ciencias, Universidade de Vigo, Ourense, Spain
[4] All-Russian Research Institute of Hydrometeorological Information—World Data Centre, Obninsk, Russian Federation
[5] Alfred Wegener Institute, Helmholtz Centre for Polar and Marine Research, Research Unit Potsdam, Germany

E-mail: martin.wegmann@giub.unibe.ch

OPEN ACCESS

RECEIVED
7 February 2015

REVISED
27 April 2015

ACCEPTED FOR PUBLICATION
28 April 2015

PUBLISHED
15 May 2015

Keywords: snow depth, Arctic warming, global change, global warming, sea ice, Siberia

Supplementary material for this article is available online

Abstract

Eurasian fall snow cover changes have been suggested as a driver for changes in the Arctic Oscillation and might provide a link between sea-ice decline in the Arctic during summer and atmospheric circulation in the following winter. However, the mechanism connecting snow cover in Eurasia to sea-ice decline in autumn is still under debate. Our analysis is based on snow observations from 820 Russian land stations, moisture transport using a Lagrangian approach derived from meteorological re-analyses. We show that declining sea-ice in the Barents and Kara Seas (BKS) acts as moisture source for the enhanced Western Siberian snow depth as a result of changed tropospheric moisture transport. Transient disturbances enter the continent from the BKS region related to anomalies in the planetary wave pattern and move southward along the Ural mountains where they merge into the extension of the Mediterranean storm track.

1. Introduction

Arctic summer sea-ice extent has declined by more than 10% per decade since the start of the satellite era (e.g. Stroeve *et al* 2011), culminating in a record low in September 2012, with the long-term trend largely attributed to anthropogenic global warming.

This results in an increasing autumn surface heat flux from the open waters to the cooler atmosphere with anomalous warming of the lower Arctic atmosphere (e.g. Overland and Wang 2010, Screen and Simmonds 2010) and important consequences for mid-latitude climate. Various mechanisms have been suggested as to how the atmosphere responds to this heat flux anomaly, starting in fall, and then into the subsequent winter season (see Vihma 2014 for a review). Honda *et al* 2009 used observations and numerical experiments to investigate the influence of Arctic sea-ice decrease on cold Eurasian winters. They argued that an October heat low over the Barents-Kara Seas (BKS) triggers a dynamical feedback, leading to increased November SLP and amplified cold advection over Central Siberia. Recently, Mori *et al* 2014 used an ensemble model approach to compare high and low sea-ice conditions and found that sea-ice reduction leads to more severe winters in central Eurasia, due to increased European blockings and resulting cold-air advection. In simulations Orsolini *et al* 2012 showed that, by December intensified surface highs were found on the American and Eurasian continents, associated with anomalous southward advection of cold polar air on their eastern sides. Contrasting the 1990–2000 and the 2001–2010 decades in re-analysis, Jaiser *et al* 2012 showed that low September sea-ice extent is associated with earlier onset of baroclinic wave activity at high latitudes, and later influenced planetary-scale wave trains extending over the North Pacific.

However, the sign and magnitude of the large-scale response is highly sensitive to the amount of sea-ice reduction and its location (Petoukhov and Semenov 2010, Rinke *et al* 2013). For example, the BKS has been suggested to be a key source region for anomalous heat fluxes and large-scale wave trains across Eurasia in winter (Inoue *et al* 2012).

Contrary to this Arctic Sea warming, North America, Europe, and East Asia have experienced anomalously cold winters with record high snowfalls and cold air outbreaks during recent winters. Such conditions have had a large impact on society and understanding the causes of such extreme events is therefore of large societal importance. While not being the only mechanism proposed, reduced summer and autumn Arctic sea-ice has been linked to atmospheric circulation changes that caused these extreme winter conditions (Honda *et al* 2009, Cohen *et al* 2014).

Francis *et al* 2009 and then Liu *et al* 2012 associated the low autumn sea-ice extent to blocking, jet stream meandering and enhanced moisture transport and snowfall in winter. Francis and Vavrus 2012 argued, based on observational evidence, for increased planetary wave amplitudes during autumn and winter in low Arctic sea-ice years, which might support the occurrence of weather extremes in mid-latitudes. Hence, the reduction in Arctic summer sea-ice could potentially increase the Eurasian autumn snowpack.

Moreover, observational as well as model studies have shown that the Eurasian autumn snowpack influences the propagation of planetary waves and the phase of the winter NAO, leading to an intensification and westward expansion of the Siberian High (Cohen *et al* 2007, Orsolini and Kvamst\o 2009, Peings *et al* 2012, Zhang *et al* 2013). Cold advection from the Arctic to Western Siberia has been shown to strengthen the Siberian high (Takaya and Nakamura 2005). Furthermore, recent studies demonstrate that initialization of snow has an impact on sub-seasonal autumn and winter forecasts (Jeong *et al* 2013, Orsolini *et al* 2013).

Finnis *et al* 2007 and more recently Stroeve *et al* 2011 linked low Arctic sea-ice in autumn to enhanced Arctic precipitation and cyclone activity, especially in the Atlantic sector. Ghatak *et al* 2012 further used a suite of dedicated model simulations with varying forcings to attribute the increase in modelled snow depth and cover over northeastern Siberia to the decreasing trend in sea-ice. Cohen *et al* 2012 qualitatively linked sea-ice loss to additional surface evaporation and earlier snowfall over high-latitude lands, consistent with estimated trends in Arctic moisture content from radiosondes and in Eurasian snow cover extent. Using a land surface model forced by observational data, Park *et al* 2013 showed increased precipitation and snow depths over northeastern Siberia in particular, associated with low autumn sea-ice extent analysed from satellite data.

However, so far no empirical, statistical or model study clearly attributed the snow increase over high-latitude land to moisture transport following specific circulation pathways originating over the ice-free parts of the Arctic Ocean. Furthermore some of these statistical studies of the sea-ice influence on winter climate are still strongly debated (e.g. Barnes 2013, Screen and Simmonds 2013). Hence, uncertainties remain in how different sea-ice anomalies influence the atmospheric circulation, either directly or through enhanced moisture. Furthermore, identifying this response is an intricate issue given the large natural variability in the cold season (i.e. Deser *et al* 2012) and inherent uncertainties arising from deficiencies in large-scale snow observations.

The goal of this study is to demonstrate the consistency between *in situ* observations of the snow pack variability over parts of Siberian and Russian Arctic regions in the early snow fall season (October, November), and sea-ice variability in the BKS region. We focus on the Siberian and Russian Arctic regions since we are using a new set of homogeneised snow observations over Russia. We calculate composites for low and high September sea-ice over the BKS of snow depths, forward trajectories out of the BKS region, and backward trajectories from high snowfall regions.

The paper is organised as follows. Section 2 describes the data and methods used. Section 3 presents the results separately for October and November. Results are discussed in section 4. Conclusions are then drawn in section 5.

2. Data and methods

2.1. Analysis framework and atmospheric circulation diagnostics

Based on HadISST sea-ice data (Rayner *et al* 2003) we defined years with high or low sea-ice in the BKS region (65–85°N, 30–90°E) in September (figure 1). In September, sea-ice reaches its annual minimum and open waters provide a strong moisture source for the cold Arctic atmosphere (Bintanja and Selten 2014). High and low ice years are defined by exceeding one standard deviation of the normalized sea-ice concentration for the timeframe of ERA-Interim 1979–2013 (see supplementary material available at stacks.iop.org/ERL/10/054015/mmedia). This results in six high sea-ice years (1980, 1981, 1989, 1998, 2002, 2003) and four low sea-ice years (1979, 1984, 1985, 2012). We then analyse snow depth, moisture transport and atmospheric circulation diagnostics for the selected years in October and November. In the following, we show the differences for low minus high September sea-ice; the significance of the differences was calculated using a t-test.

The following atmospheric circulation diagnostics were calculated from ERA-Interim (Dee *et al* 2011): Omega (vertical wind speed) at 700 hPa, wind at 700 hPa, mean sea level pressure (SLP), 500 hPa geopotential height, integrated water vapour transport, snowfall, 2 m temperatures, variance of 2–7 day band-passed daily SLP.

2.2. Snow cover data

Regular snow observations have been conducted at Russian meteorological stations since 1882. Daily

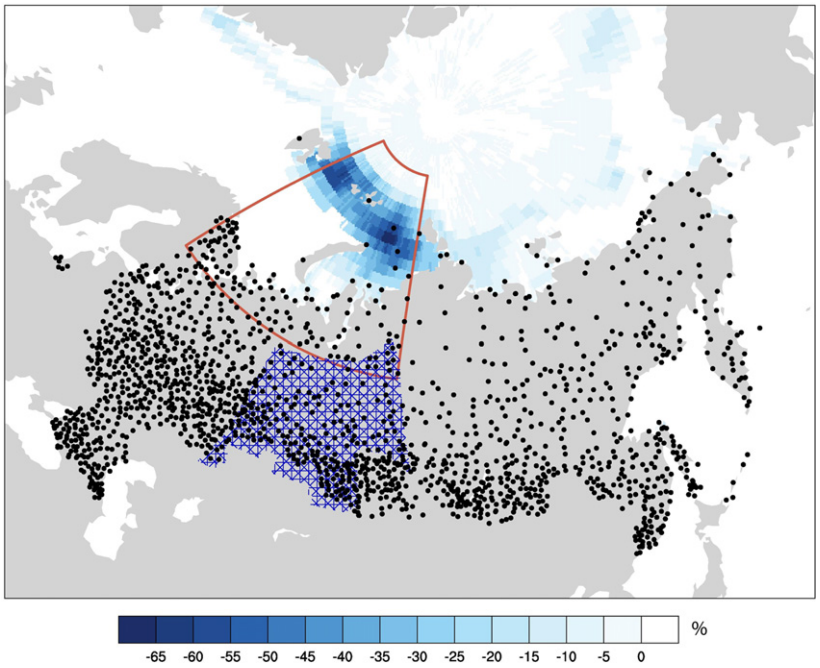

Figure 1. Map showing the positions of the 820 snow cover stations (black dots), with the Barents/Kara Sea (BKS) and the 'southwestern Siberia' regions highlighted (red frame and blue crossing, respectively). Blue shading shows the composite of HadISST October and November sea-ice concentration anomalies of low minus high sea-ice years.

snow observations at meteorological stations include snow depth measurements, determination of the snow cover in an area around a meteorological station and determination of the snow cover characteristics. This study uses time series of daily snow depths for 820 Russian meteorological stations, distributed as shown on figure 1. The time series are prepared by RIHMI-WDC. Meteorological data sets are automatically checked for quality control. Since the procedure of snow observations changed in the past, particular attention was given to the removal of all possible sources of inhomogeneity in the data. However, there have been no changes in the observation procedures since 1965. Only the period 1979–2012 was used in the study.

For definition of snow covered regions in this paper, we used as a primary step Russian national climate monitoring regions as defined by Alisov 1956 and by Bulygina *et al* 2010. The primary division to regions considers 18 regions over all the territory of Russia, which describe all the variety of climate conditions and, within the region, have similar environmental conditions. This includes similar landscapes, meteorological conditions, vegetation types and more. Based on an analysis of spatial distributions of a number of climate characteristics, including snow cover characteristics, that involved sets of more than 600 meteorological stations, these 18 primary regions were then merged into nine quasi-homogeneous regions of Russian territory. Here we chose one of those regions as the main region of interest, namely the '*southwestern Siberia*', *hereafter SW-Siberia,* region (highlighted in blue crossing in figure 1).

We use monthly maximum snow depth instead of mean values because it reflects the process of snow accumulation (snow depth is a cumulative and highly inertial characteristic of climate system). It is especially essential for autumn months when the main processes of snow accumulation occurs over the territories of Russia.

2.3. Lagrangian modeling

The Lagrangian analyses in this work has been developed using the model FLEXPART V9.0 and is based on the method developed by Stohl and James 2004, 2005. This model uses ERA-Interim reanalysis data to track changes in atmospheric moisture along trajectories. The model considers the atmosphere divided into a large number of particles, which are advected using the three dimensional wind data. The increases (evaporation e) and decreases (precipitation p) in moisture along any trajectory can be calculated through changes in (specific humidity q) with time ($e\text{-}p = m\mathrm{d}q/\mathrm{d}t$), with ($m$) being the mass of the particle. By summing (e-p) for all particles residing in the atmospheric column over an area we can obtain the total (E-P) field. The number of particles reaching a target area from a source can be different for different periods. However, the global amount of particles stays the same at all times.

In this work we first try to establish a relation between the retreat of sea-ice in the BKS region and

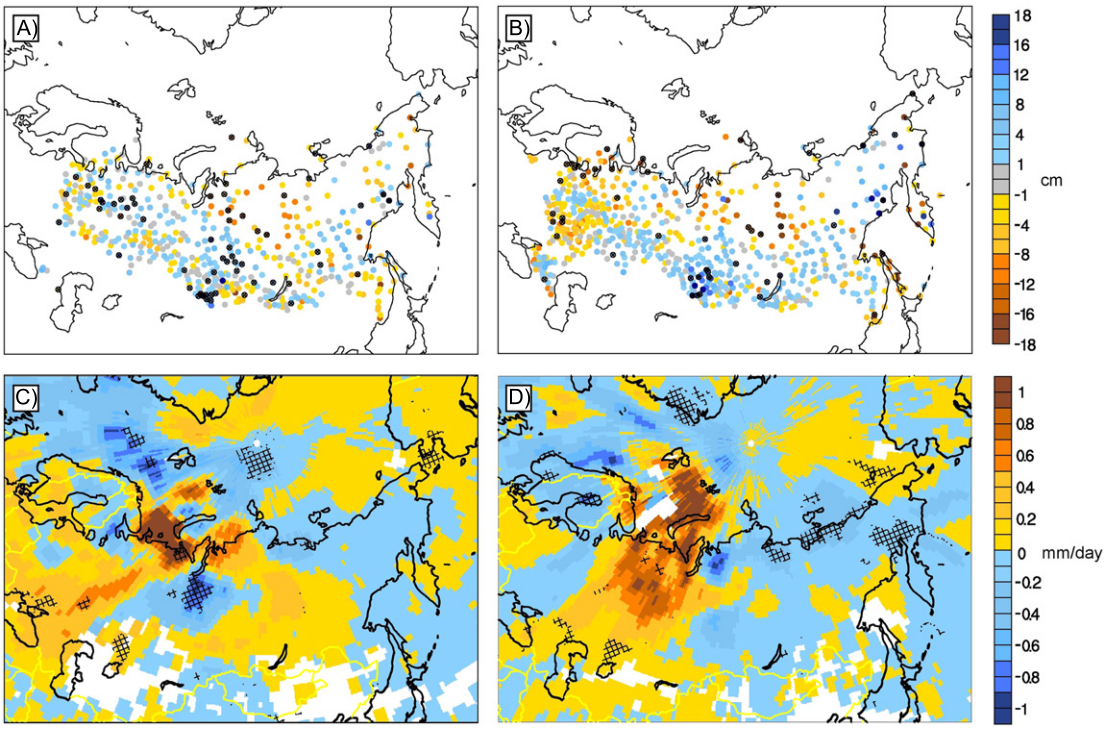

Figure 2. Differences between low and high BKS September sea-ice in station snow depth (cm) for (A) October and (B) November. *E-P* differences (mm day^{-1}) from forward trajectories starting in the BKS region for (C) October and (D) November. Cross hatched areas and crossed stations represent 90% Student's t-test significance level.

the precipitation over the region 'southwestern Siberia' (figure 1). This is done by a forward analysis considering only particles starting in the BKS region and following the particles over a period of three days. Areas where particles from this region lose moisture are represented by a negative value on *E-P* field. Furthermore, a backward trajectory analysis is carried out where particles arriving over 'southwestern Siberia' are tracked backwards to their region of origin over a period of three days. In this way we determine the regions where particles arriving in 'southwestern Siberia' have picked up moisture. In this case, the grid points where $E\text{-}P > 0$ represent areas where particles gain moisture.

Full details on the methods in the forward or backward modes can be found in Nieto *et al* 2008 or Gimeno *et al* 2010 respectively, and a comparison of the Lagrangian technique with other methods for derivation of moisture sources can be found in Gimeno *et al* 2012.

3. Results

3.1. October

The composite difference of *in situ* snow observations in figure 2 shows that Octobers in years with low BKS sea-ice have significantly higher snow depths in Southern Siberia, and also in some coastal areas of the Far East and Northern Volga, with the first being the most striking region of positive anomalies. Forward trajectories composite difference also indicate, that during low ice years, air parcels which start over the BKS tend to lose more moisture over the Urals and the Far East. The maximum loss difference is located in an area with its western boundary over the Urals and continuing to south-west Siberia, whereas moisture loss minima are found at the coastal areas of the Northwest and at the western Russian border (figure 2).

We now consider composite differences of a variety of dynamical diagnostics derived from ERA-Interim (figure 3). We can see in figure 3 (second row) that the region of the loss maximum is located at the northern edge of a strong negative SLP anomaly, which is bound to the north and west by anti-cyclonic anomalies, the latter centered south of Scandinavia. Positive 2 m temperature anomalies are found over the open waters of the BKS while there are only weak temperature anomalies over continental Russia (also figure 3, second row). At the south-eastern flank of the negative SLP anomaly an increase of vertical uplift can be observed (figure 3, first row). The opposite is true for areas of positive SLP anomalies. Regions with strongly enhanced (decreased) vertical uplift fit very well with positive (negative) snow depth from the independent *in situ* measurements (figure 2) and with the snowfall anomalies from re-analyses (figure 3, first row).

The composite difference of 500 hPa geopotential height and SLP (figure 3) reveals a northern

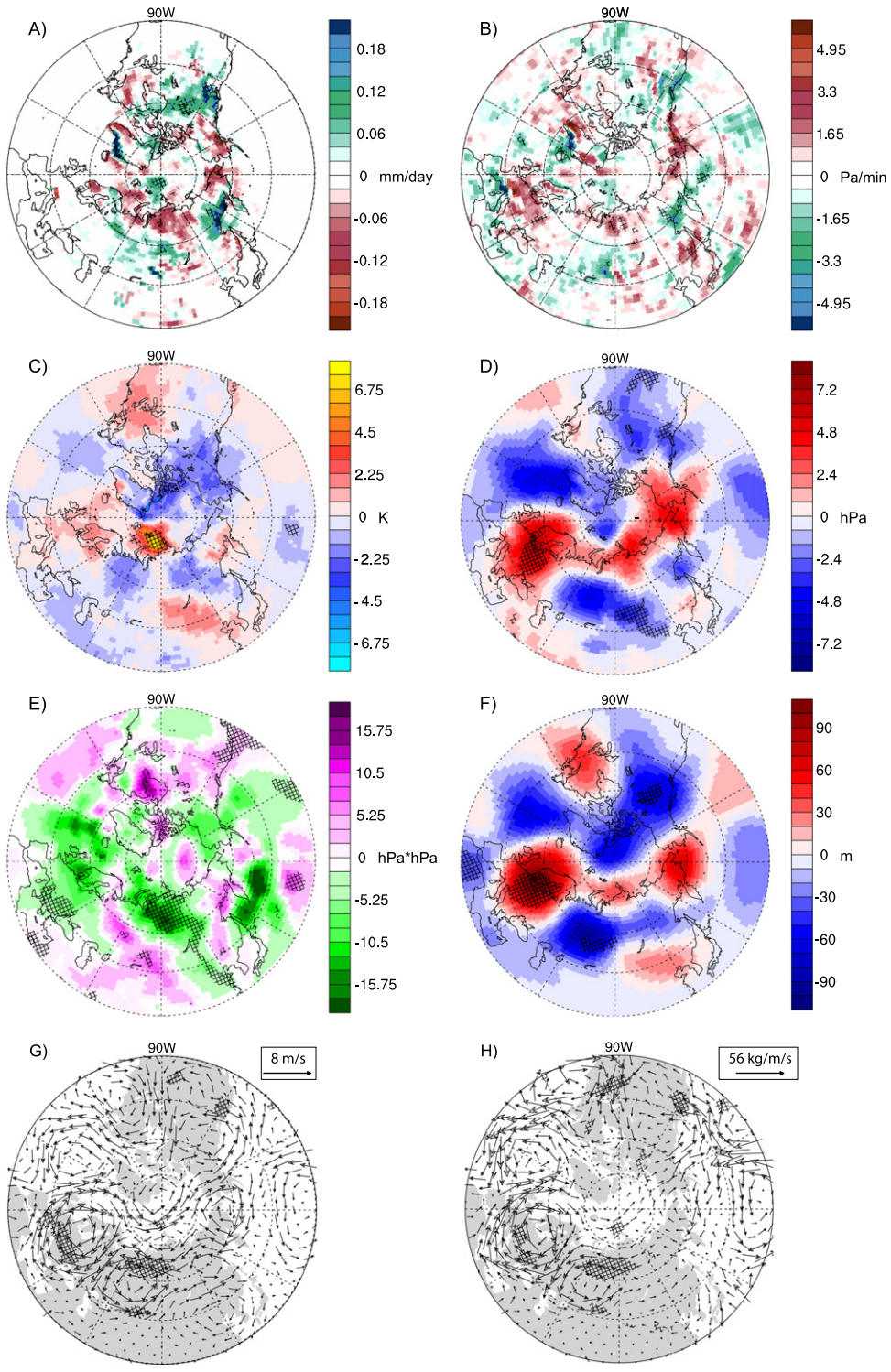

Figure 3. Difference between low and high sea-ice years in the Barents Kara Sea region for (A) snow fall (mm day^{-1}), (B) 700 hPa Omega (Pa min^{-1}), (C) 2 m temperature (K), (D) SLP (hPa), (E) and 2–7 day 247 bandpassed SLP variance (hPa^2), (F) geopotential height at 500 hPa (m), (G) 700 hPa wind (m s^{-1}), (H) integrated water vapour transport (kg m^{-1} s^{-1}) for October. Cross hatched areas represent 90% Student´s t-test significance level.

hemispheric barotropic wavetrain pattern in October. While both low and high sea-ice years show a circumpolar wave train, the low sea-ice wavetrain has a higher wavenumber (see supplementary material available at stacks.iop.org/ERL/10/054015/mmedia). Strong blocking is found over northern Europe and negative geopotential height anomalies dominate over the Ural Mountains and Western Siberia. Moisture and air mass transport over Central Russia is influenced by the cyclonic SLP anomaly to the west. The atmosphere *E-P* anomalies are positive over the warmer, open sea at the western flank of the cyclonic anomaly, as well as

over the eastern flank due to the dry, continental origin of the airmasses. Bandpassed SLP variance (figure 3) shows increased storm activity entering the Central Russia land areas through a small sector from the BKS. Hence storm are veering abruptly southward along the Urals, and areas with maximum bandpassed SLP variance fit very well with positive snow depth and snowfall anomalies.

The source of moisture can be addressed by means of the backward trajectory analysis. Backward trajectories arriving in SW-Siberia show that there are several main climatological moisture source regions for the snow falling in that region (figure 5, top row): first and foremost the large open water areas to the West, namely the Mediterranean and the North Atlantic. Furthermore, the Black Sea, Caspian Sea and the BKS region act as climatological moisture source. During low sea-ice years (figure 5, bottom row), it appears that air parcels arriving in SW-Siberia have picked up more moisture over the BKS region as opposed to high sea-ice years. This is consistent with enhanced evaporation over the low sea-ice areas (assuming no precipitation changes). A third moisture source during low sea-ice years is the Balkan region. Conversely, a region east of the southern Urals appears as a more important moisture source for high sea-ice years (figure 5). However, the importance of moisture sources can only be stated in relative terms for backward trajectory anomalies.

3.2. November

For November, the analysis of snow observations reveals similar anomalies as for October. Strong positive anomalies in Southern Siberia between Lake Balkash and Lake Baikal, positive anomalies in the Far East, now more inland than in October, coexist with significant decrease of snow depth mainly between Lake Baikal and the Arctic coast as well as towards the western border of Russia (figure 2).

Forward trajectories in FLEXPART indicate that air parcels starting over the Barents/Kara Seas tend to loose less moisture over Western Russia than during high ice years. The anticyclonic pressure anomaly over this region shuffles more continental airmasses around its core causing the atmosphere to loose less moisture along the northern and eastern flank (figure 4). Over most of Siberia and the Far East, air parcels lose more moisture in low sea-ice years. A very strong moisture loss is found at the Arctic Coast in Northern Siberia, a region where SLP is low and vertical uplift is increased, but snow anomalies are (still) negative. Moreover, positive 2 m temperature anomalies reach from the BKS inland and cover the Siberian and Far East Arctic coast. However, ERA-INTERIM indicates increased snowfall in this area (figure 4). Increased uplift and positive snowfall anomalies fit in general very well over the plotted domain.

Large-scale circulation wise, composites of 500 hPa geopotential height and SLP for low minus high sea-ice in the Barents/Kara Seas show a baroclinic pattern (figure 4). A weaker blocking occurs over European Russia and negative SLP anomalies over the northern North Atlantic appear. Both, at the surface and in the middle troposphere, the positive pressure anomalies along the Russian Arctic coast in October vanish, and more cylonic systems prevail. This opens an entry passage for a direct storm track coming from the BKS passing east of the Urals to Central Siberia and Asia. Again, areas of maximum bandpassed SLP variance match regions of positive snowfall, negative omega as well as positive snow depth anomalies from *in situ* observations. In this case, Central and Southern Siberia is pinched between an anti-cyclonic anomaly to the west and and cyclonic anomaly to the east. In the Far East, storm systems are shifted from the Pacific to Arctic areas north of Kamchatka, a region with increased moisture loss and snowfall (figure 4).

The November composite difference of backward trajectories for SW-Siberia shows again two relatively enhanced moisture source regions in low sea-ice years: the Kara Sea and the northern surroundings of the Caspian Sea. Compared to October, the Black Sea and the Balkan region no longer appear as significantly enhanced sources (figure 5).

4. Discussion

Although small in sample size, our results indicate a significant increase of observed Siberian snow depth during low sea-ice years.

Our analysis focuses on moisture transport resulting from Hori *et al* (2011) sea-ice decline in the BKS, which allows us to specify regions of interest for the FLEXPART trajectories and snow depth observations. Open waters in the BKS have been shown to increase the diabatic heating of the atmosphere (Sato *et al* 2014), which amplifies baroclinic cyclones and might induce a remote atmospheric response by triggering stationary Rossby waves (Honda *et al* 2009).

Consistent with the results, our analysis shows increased cold air advection from the north from the BKS region over western Russia and the Urals in October in low sea-ice years. This cold air convection persists in November, but is located further to the East. Snow cover anomalies then may further amplify the Siberian high through radiative and thermodynamic effects (Cohen *et al* 2012, Orsolini *et al* 2013). In fact, similar composited plots for December and January show a strengthening of the Siberian high following low sea-ice conditions during fall (see supplementary material available at stacks.iop.org/ERL/10/054015/mmedia), indicating that the anomalous northerly advection continues to build a negative 2 m temperature anomaly, in agreement with Hori *et al* 2011.

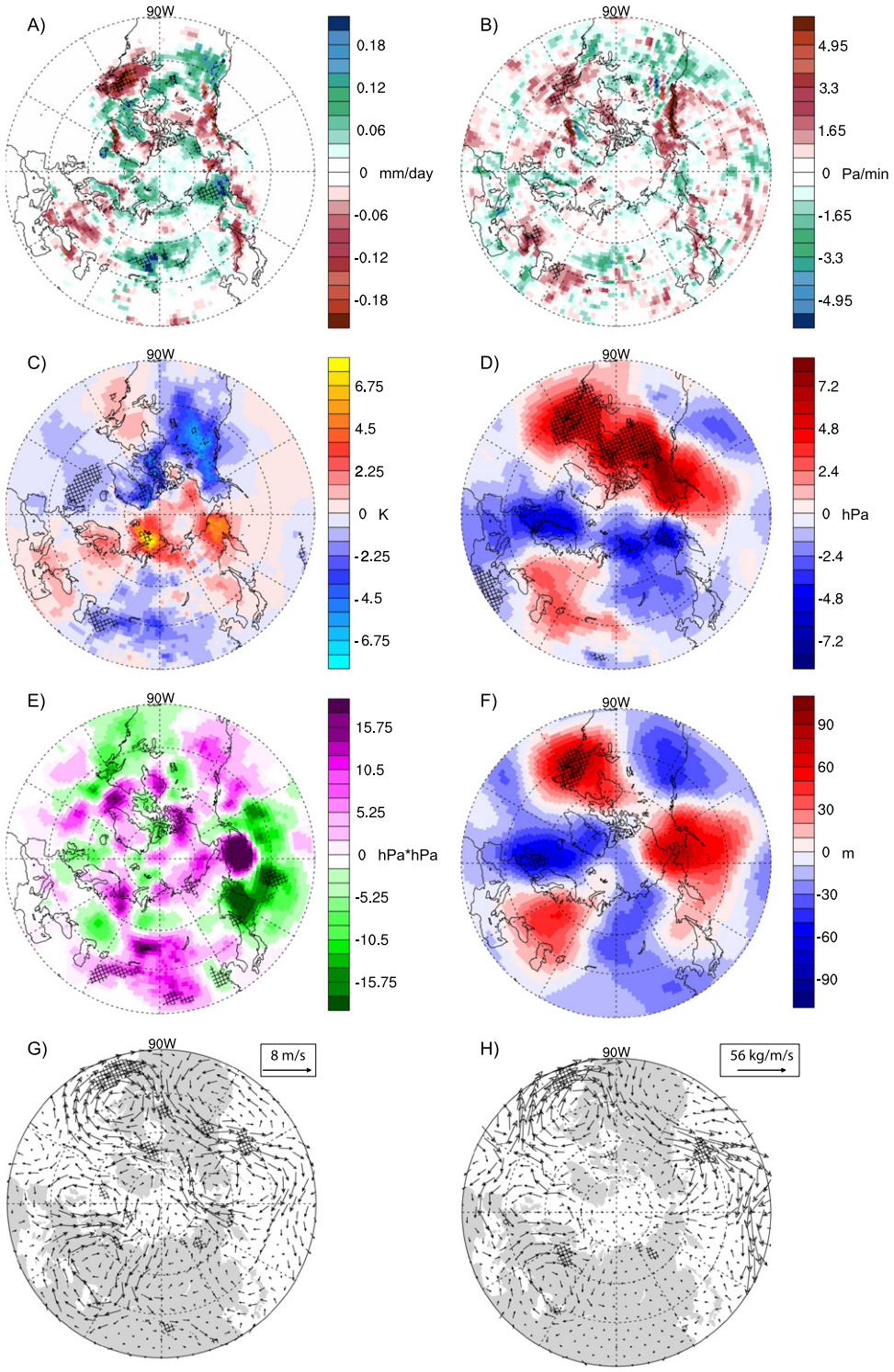

Figure 4. Difference between low and high sea-ice years in the Barents Kara Sea region for (A) snow fall (mm day^{-1}), (B) 700 hPa Omega (Pa min^{-1}), (C) 2 m temperature (K), (D) SLP (hPa), (E) and 2–7 day bandpassed SLP variance (hPa^2), (F) geopotential height at 500 hPa (m), (G) 700 hPa wind (m s^{-1}), (H) integrated water vapour transport (kg m^{-1} s^{-1}) for November. Cross hatched areas represent 90% Student´s t-test significance level.

In agreement with these studies, we found strengthened European blocking and increased wave numbers at 500 hPa. Moreover, our results show enhanced storm activity originating in the BKS with disturbances entering the continent through a small sector over the BKS, steered in October by a Scandinavia block and a low to the East and extending to Central Russia. In case of the strong snow depth increase during October in SW-Siberia, enhanced frontal activity on the southeastern flank of the cyclonic anomaly is a possible trigger for the increased vertical uplift. Maxima in storm activity trigger increasing

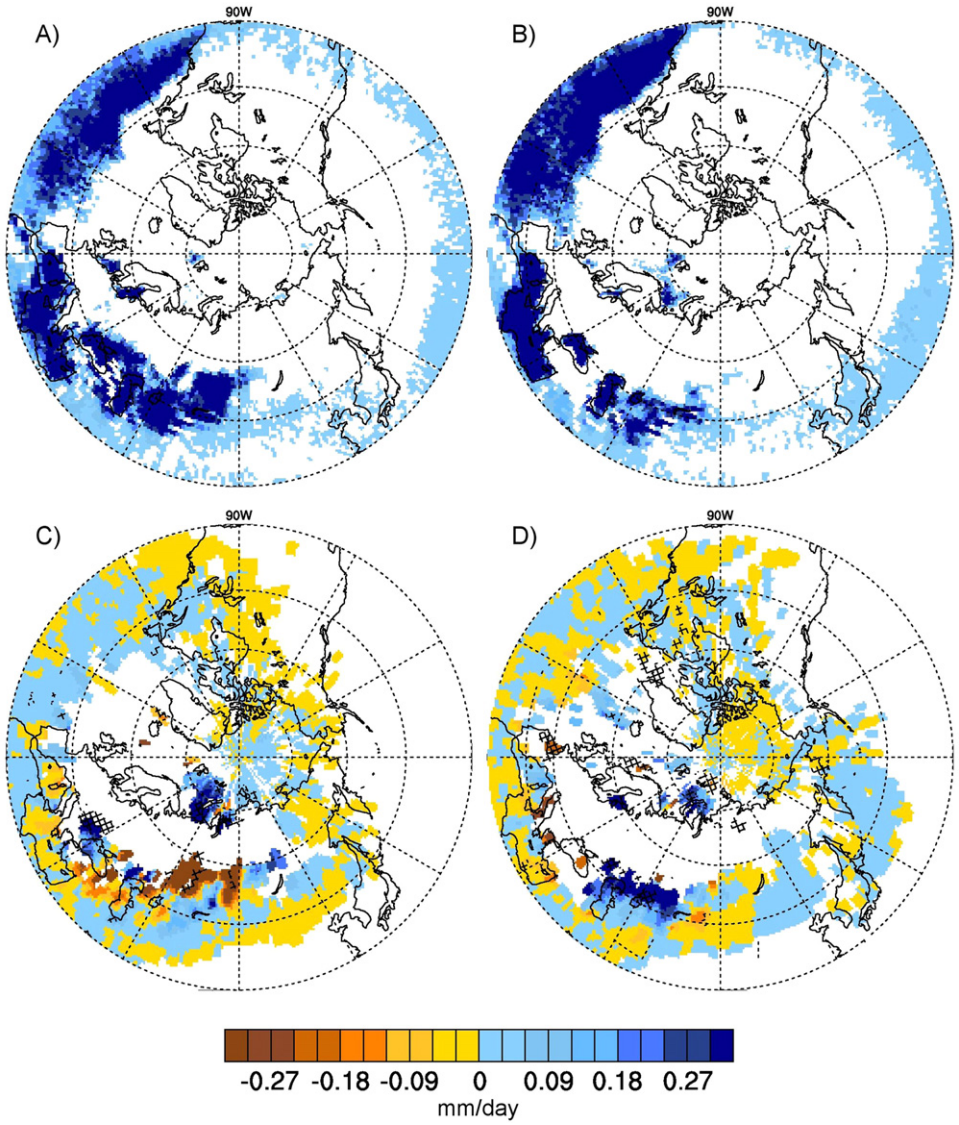

Figure 5. (A) Climatological (1980–2012) moisture sources and (C) composite differences in the moisture gain for backward trajectories starting in southwestern Siberia' (region of relatively high snow depth in low ice years) for October. B and D show the same for November. Cross hatched areas represent 90% Student´s test significance level for anomaly plots.

uplift, often accompanied by positive snowfall and snow depth anomalies. Forward and backward FLEXPART analysis support the idea that decreasing Arctic sea-ice cover in the BKS region is a main source and an important factor for continental snow accumulation, especially so in SW-Siberia. Over other areas, like the Pacific coast of the Far East., a combination of frontal activity and coastal convergence causes upward vertical wind anomalies and snow accumulation. This initial snowpack anomaly is then influencing the evolution of the November snow pack.

However, no direct link between Lagrangian moisture loss and snow accumulation in observations can be made. FLEXPART computes moisture loss in a diverse way, including cloud evolution and related processes. Additionally, surface temperature conditions impacts on snowmelt and snow depth cannot be accounted for in the FLEXPART analysis. We needed to use a combination of Lagrangian and Eularian approaches to analyse snow depth evolution.

In this study, focused on early autumn, we were not able to determine the circulation response to BKS sea-ice anomalies, as it appears masked or embedded in the circumglobal wavetrain (see supplementary material available at stacks.iop.org/ERL/10/054015/mmedia). Kim *et al* 2014 recently looked at BKS sea-ice retreat influence on the atmosphere in re-analyses and model data. They found that the response in the mid-tropospheric circulation becomes apparent only by December, inducing cold wintertime anomalies over northern Eurasia. Our paper complements their study in that we investigated the leading season to that signal.

Future studies are needed to investigate further the links and impacts of the rapidly changing Arctic climate. Ensemble model simulations for past and current conditions may increase the statistical

significance of the proposed physical links, connecting reduced sea-ice and Eurasian surface conditions. Future climate model simulations (Deser *et al* 2010, Callaghan *et al* 2011) indicate an increase in snow water equivalent over Siberia due to decreasing Arctic sea-ice.

5. Summary

An extensive, dense snow depth observation dataset was analyzed to examine autumn snow depth evolution in Russia during the recent Arctic warming period. Evidence was found for an increase of SW-Siberian snow depth in years of low sea-ice in the BKS region. Backward trajectories from FLEXPART originating in that region indicate the BKS as an important moisture source.

Eulerian diagnostics from ERA-INTERIM show an increased atmospheric wavenumber and meridional circulation during low sea-ice years. Besides promoting cold air advection from the Arctic Ocean into the Eurasian continent, these circulation changes are accompanied by an intensified storm track into SW-Siberia. Anomalies in snowfall generally agree well with snow depth observations and are often found over regions with strong changes in atmospheric lift. Both the southeastern flanks of cyclonic anomalies and the coastal sea breeze convergence are major triggers for such upward vertical motions. However, surface conditions are critical for the conversion of snowfall into snow depth. Reversely, the SW-Siberian snow depth increase is subsequently influences temperature and positive pressure tendency later in the cold season.

These findings are consistent with several former studies and consequently underline the importance of Arctic climate change for lower latitude regions. The question remains open if future sea-ice melting will lead to the same results, however modeling studies point towards a similar mechanism. To further quantify the impacts of those environmental changes, it is critical to continue a dense, high quality snow depth observation network in the coming decades. Moreover, extending the study to other sea-ice loss areas and to other continental areas of the Northern Hemisphere might give insight into the regional differences of the 'warm Arctic, cold continent' model.

Acknowledgements

The authors acknowledge funding by the European ERAnet.RUS programme, especially within the project ACPCA. The EPhysLab acknowledges the funding of the TRAMO project by the Spanish MINECO and FEDER.

References

Alisov B P 1956 *Climate of the USSR* (Moscow: Moscow University)
Barnes E A 2013 Revisiting the evidence linking Arctic amplification to extreme weather in midlatitudes *Geophys. Res. Lett.* **40** 4734–9
Bintanja R and Selten F M 2014 Future increases in Arctic precipitation linked to local evaporation and sea-ice retreat *Nature* **509** 479–82
Bulygina O N, Groisman P Y, Razuvaev V N and Radionov V F 2010 Snow cover basal ice layer changes over Northern Eurasia since 1966 *Environ. Res. Lett.* **5** 015004
Callaghan T V, Johansson M, Prowse T D, Olsen M S and Reiersen L O 2011 Arctic cryosphere: changes and impacts *Ambio* **40** 3–5
Cohen J, Barlow M, Kushner P J and Saito K 2007 Stratosphere–troposphere coupling and links with Eurasian land surface variability *J. Clim.* **20** 5335–43
Cohen J, Screen J A, Furtado J C, Barlow M, Whittleston D, Coumou D, Francis J, Dethloff K, Entekhabi D and Overland J 2014 Recent Arctic amplification and extreme mid-latitude weather *Nat. Geosci.* **7** 627–37
Cohen J L, Furtado J C, Barlow M A, Alexeev V A and Cherry J E 2012 Arctic warming, increasing snow cover and widespread boreal winter cooling *Environ. Res. Lett.* **7** 014007
Dee D P *et al* 2011 The ERA-Interim reanalysis: configuration and performance of the data assimilation system *Q. J. R. Meteorol. Soc.* **137** 553–97
Deser C, Phillips A, Bourdette V and Teng H 2012 Uncertainty in climate change projections: the role of internal variability *Clim. Dyn.* **38** 527–46
Deser C, Tomas R, Alexander M and Lawrence D 2010 The seasonal atmospheric response to projected Arctic sea ice loss in the late twenty-first century *J. Clim.* **23** 333–51
Finnis J, Holland M M, Serreze M C and Cassano J J 2007 Response of Northern Hemisphere extratropical cyclone activity and associated precipitation to climate change, as represented by the Community Climate System Model *J. Geophys. Res.: Biogeosci.* **112** G04S42
Francis J A, Chan W, Leathers D J, Miller J R and Veron D E 2009 Winter Northern Hemisphere weather patterns remember summer Arctic sea-ice extent *Geophys. Res. Lett.* **36** L07503
Francis J A and Vavrus S J 2012 Evidence linking Arctic amplification to extreme weather in mid-latitudes *Geophys. Res. Lett.* **39** L06801
Ghatak D, Deser C, Frei A, Gong G, Phillips A, Robinson D A and Stroeve J 2012 Simulated Siberian snow cover response to observed Arctic sea ice loss, 1979–2008 *J. Geophys. Res.: Atmos.* **117** D23108
Gimeno L, Drumond A, Nieto R, Trigo R M and Stohl A 2010 On the origin of continental precipitation *Geophys. Res. Lett.* **37** L13804
Gimeno L, Stohl A, Trigo R M, Dominguez F, Yoshimura K, Yu L, Drumond A, n.-Q. A. M. i. a. Dur\'a and Nieto R 2012 Oceanic and terrestrial sources of continental precipitation *Rev. Geophys.* **50** RG4003
Honda M, Inoue J and Yamane S 2009 Influence of low Arctic sea-ice minima on anomalously cold Eurasian winters *Geophys. Res. Lett.* **36** L08707
Hori M E, Inoue J, Kikuchi T, Honda M and Tachibana Y 2011 Recurrence of intraseasonal cold air outbreak during the 2009/2010 winter in Japan and its ties to the atmospheric condition over the Barents-Kara Sea *SOLA* **7** 25–8
Inoue J, Hori M E and Takaya K 2012 The role of Barents Sea ice in the wintertime cyclone track and emergence of a warm-Arctic cold-Siberian anomaly *J. Clim.* **25** 2561–8
Jaiser R, Dethloff K, Handorf D O R, Rinke A and Cohen J 2012 Impact of sea ice cover changes on the Northern Hemisphere atmospheric winter circulation *Tellus* A **64** 11595
Jeong S-J, Ho C-H, Kim B-M, Feng S and Medvigy D 2013 Non-linear response of vegetation to coherent warming over northern high latitudes *Remote Sens. Lett.* **4** 123–30

Kim B M, Son S W, Min S K, Jeong J H, Kim S J, Zhang X D, Shim T and Yoon J H 2014 Weakening of the stratospheric polar vortex by Arctic sea-ice loss *Nat. Commun.* **5** 4646

Liu J, Curry J A, Wang H, Song M and Horton R M 2012 Impact of declining Arctic sea ice on winter snowfall *Proc. Natl Acad. Sci. USA* **109** 4074–9

Mori M, Watanabe M, Shiogama H, Inoue J and Kimoto M 2014 Robust Arctic sea-ice influence on the frequent Eurasian cold winters in past decades *Nat. Geosci.* **7** 869–73

Nieto R, Gallego D, Trigo R, Ribera P and Gimeno L 2008 Dynamic identification of moisture sources in the Orinoco basin in equatorial South America *Hydrol. Sci. J.* **53** 602–17

Orsolini Y J and Kvamst\o N G 2009 Role of Eurasian snow cover in wintertime circulation: decadal simulations forced with satellite observations *J. Geophys. Res.: Atmos.* **114** D19108

Orsolini Y J, Senan R, Balsamo G, Doblas-Reyes F J, Vitart F, Weisheimer A, Carrasco A and Benestad R E 2013 Impact of snow initialization on sub-seasonal forecasts *Clim. Dyn.* **41** 1969–82

Orsolini Y J, Senan R, Benestad R E and Melsom A 2012 Autumn atmospheric response to the 2007 low Arctic sea ice extent in coupled ocean–atmosphere hindcasts *Clim. Dyn.* **38** 2437–48

Overland J E and Wang M 2010 Large-scale atmospheric circulation changes are associated with the recent loss of Arctic sea ice *Tellus* A **62** 1–9

Park H, Walsh J E, Kim Y, Nakai T and Ohata T 2013 The role of declining Arctic sea ice in recent decreasing terrestrial Arctic snow depths *Polar Sci.* **7** 174–87

Peings Y, Saint-Martin D and Douville H 2012 A numerical sensitivity study of the influence of Siberian snow on the northern annular mode *J. Clim.* **25** 592–607

Petoukhov V and Semenov V A 2010 A link between reduced Barents-Kara sea ice and cold winter extremes over northern continents *J. Geophys. Res.: Atmos.* **115** D21111

Rayner N A, Parker D E, Horton E B, Folland C K, Alexander L V, Rowell D P, Kent E C and Kaplan A 2003 Global analyses of sea surface temperature, sea ice, and night marine air temperature since the late nineteenth century *J. Geophys. Res.: Atmos.* **108** 4407

Rinke A, Dethloff K, Dorn W, Handorf D and Moore J C 2013 Simulated Arctic atmospheric feedbacks associated with late summer sea ice anomalies *J. Geophys. Res.: Atmos.* **118** 7698–714

Sato K, Inoue J and Watanabe M 2014 Influence of the Gulf stream on the Barents Sea ice retreat and Eurasian coldness during early winter *Environ. Res. Lett.* **9** 084009

Screen J A and Simmonds I 2010 Increasing fall-winter energy loss from the Arctic Ocean and its role in Arctic temperature amplification *Geophys. Res. Lett.* **37** L16707

Screen J A and Simmonds I 2013 Exploring links between Arctic amplification and mid-latitude weather *Geophys. Res. Lett.* **40** 959–64

Stohl A and James P 2004 A Lagrangian analysis of the atmospheric branch of the global water cycle: I. Method description, validation, and demonstration for the August 2002 flooding in central Europe *J. Hydrometeorol.* **5** 656–78

Stohl A and James P 2005 A Lagrangian analysis of the atmospheric branch of the global water cycle: II. Moisture transports between Earth's ocean basins and river catchments *J. Hydrometeorol.* **6** 961–84

Stroeve J C, Maslanik J, Serreze M C, Rigor I, Meier W and Fowler C 2011 Sea ice response to an extreme negative phase of the Arctic Oscillation during winter 2009/2010 *Geophys. Res. Lett.* **38** L02502

Takaya K and Nakamura H 2005 Mechanisms of intraseasonal amplification of the cold Siberian high *J. Atmos. Sci.* **62** 4423–40

Vihma T 2014 Effects of Arctic Sea ice decline on weather and climate: a review *Surv. Geophys.* **35** 1175–214

Zhang X, He J, Zhang J, Polyakov I, Gerdes R U D, Inoue J and Wu P 2013 Enhanced poleward moisture transport and amplified northern high-latitude wetting trend *Nat. Clim. Change* **3** 47–51